

# Resonance Raman Investigations of Cytochrome P450<sub>cam</sub> Complexed with Putidaredoxin

Masashi Unno,<sup>†,§</sup> James F. Christian,<sup>†</sup> David E. Benson,<sup>‡</sup> Nancy C. Gerber,<sup>‡</sup> Stephen G. Sligar,<sup>‡</sup> and Paul M. Champion<sup>\*,†</sup>

Contribution from the Department of Physics, Northeastern University, Boston, Massachusetts 02115, and Departments of Biochemistry and Chemistry, University of Illinois at Urbana–Champaign, Urbana, Illinois 61801

Received October 31, 1996<sup>⊗</sup>

**Abstract:** We have performed resonance Raman and optical absorption studies on ferric cytochrome P450<sub>cam</sub> complexed with oxidized putidaredoxin. Optical absorption and resonance Raman measurements demonstrate that this complexation shifts the spin-state equilibrium of P450<sub>cam</sub> to the low-spin form. In the resonance Raman spectra, the  $\nu_3$  heme skeletal mode characteristic of low-spin P450<sub>cam</sub> intensifies upon complexation with putidaredoxin. Its frequency is indistinguishable to that of the usual low-spin species, indicating that this low-spin form originates from a water-bound, hexacoordinate heme. This observation suggests that putidaredoxin binding affects the distal side of P450<sub>cam</sub> and allows water entry into the heme pocket. We also examined the effects of putidaredoxin binding on the heme axial ligand (Fe–S) stretching mode. The binding of putidaredoxin upshifts the mode by  $\sim 3$  cm<sup>-1</sup>. Investigations of the Fe–S mode for the Thr252  $\rightarrow$  Ala distal pocket mutant and P450<sub>cam</sub> bound to various camphor analogues demonstrate that the frequency of the  $\nu_{\text{Fe-S}}$  is sensitive to distal pocket water. The water lowers the Fe–S stretching frequency by  $\sim 1$  cm<sup>-1</sup>, demonstrating that the putidaredoxin-induced  $\sim 3$ -cm<sup>-1</sup> increase in the Fe–S stretching frequency is not simply caused by the increased hydration of the heme pocket. We also found that the Fe–S frequency is increased by  $\sim 0.5$  cm<sup>-1</sup> in the presence of high salt concentrations. This result suggests that the shielding of positive charges at the proximal face of P450<sub>cam</sub> leads to an increased  $\nu_{\text{Fe-S}}$  frequency. The salt effect is consistent with the observation that the binding of negatively charged putidaredoxin at the proximal side of the enzyme also increases the  $\nu_{\text{Fe-S}}$  frequency. Taken together, these results strongly suggest that electrostatic shielding of charged groups on the proximal face of P450<sub>cam</sub> takes place when putidaredoxin binds and contributes to the observed upshift of the Fe–S mode.

## Introduction

The cytochrome P450 class of enzymes is involved in a wide range of biological oxidations, including epoxidations, hydroxylations, and heteroatom oxidations. The most distinctive feature in the structure of cytochrome P450 is the coordination of a thiolate anion, from the proximal cysteine residue, to the heme iron as a fifth ligand. Cytochrome P450<sub>cam</sub> from the bacterium *Pseudomonas putida* (CYP101) catalyzes the regio- and stereospecific hydroxylation of its substrate, *d*-camphor, at the 5-*exo* position.<sup>1</sup> Because the structure of the P450<sub>cam</sub> enzyme has been fairly well-defined by many spectroscopic studies<sup>2</sup> and also X-ray crystallography,<sup>3</sup> it has become a prototype for the entire P450 family of enzymes. In its reaction cycle, P450<sub>cam</sub> requires two electrons to yield product (5-*exo*-hydroxycamphor), and water, from molecular oxygen and the substrate, camphor. The iron–sulfur (2Fe/2S) protein, putidaredoxin (Pd), transfers these electrons from the FAD-containing putidaredoxin reductase to P450<sub>cam</sub> in two discrete steps.

The electron transfer reaction of Pd with P450<sub>cam</sub> has been extensively studied. Stayton et al. found that Pd competitively inhibits cytochrome *b*<sub>5</sub>/P450<sub>cam</sub> association, and suggested that P450<sub>cam</sub> binds cytochrome *b*<sub>5</sub> and Pd at the same or overlapping

sites.<sup>4</sup> With the availability of the P450<sub>cam</sub> and cytochrome *b*<sub>5</sub> structures, they performed computer modeling and proposed that Pd approaches P450<sub>cam</sub> from the proximal face with the interaction being guided by charge–charge coupling. Their model suggested that the basic P450<sub>cam</sub> residues Arg72, Arg112, Lys344, and Arg364 contribute to the electrostatic interactions. Subsequently, Stayton and Sligar showed that mutations of Arg72 and Lys344, to either glutamate or glutamine, result in a modest lowering (20–60%) of binding affinities for Pd to P450<sub>cam</sub>.<sup>5</sup> Recent site-directed mutagenesis studies on P450<sub>cam</sub> provide further evidence for the involvement of one of these basic residues in forming the diprotein complex.<sup>6</sup> A variety of mutations at the Arg112 position showed that charge neutralization of this residue leads to a dramatic decrease in enzymatic activity. Furthermore, these mutations cause a  $>600$ -fold increase of the dissociation constant  $K_d$  for the complex formation reaction between ferric P450<sub>cam</sub> and reduced Pd.<sup>6c</sup> These studies with site-directed mutagenesis strongly suggest that Pd binds to the proximal surface of P450<sub>cam</sub>.

In addition to its redox role, Pd has also been shown to act as an effector in P450<sub>cam</sub> catalysis. The oxygenated P450<sub>cam</sub> is incapable of turnover in the absence of Pd, and a kinetic analysis suggests that the diprotein complex is the active species for camphor hydroxylation.<sup>7</sup> In accordance with the idea of the

\* Author to whom correspondence should be addressed.

<sup>†</sup> Northeastern University.

<sup>‡</sup> University of Illinois.

<sup>§</sup> Present Address: Institute for Chemical Reaction Science, Tohoku University, Sendai 980, Japan.

<sup>⊗</sup> Abstract published in *Advance ACS Abstracts*, July 1, 1997.

(1) Ortiz de Montellano, P. R. *Cytochrome P450 Structure, Mechanism, and Biochemistry*; Plenum Press: New York, 1995.

(2) Dawson, J. H.; Sono, M. *Chem. Rev.* **1987**, *87*, 1255–1276.

(3) Poulos, T. L.; Raag, R. *FASEB J.* **1992**, *6*, 674–679.

(4) Stayton, P. S.; Poulos, T. L.; Sligar, S. G. *Biochemistry* **1989**, *28*, 8201–8205.

(5) Stayton, P. S.; Sligar, S. G. *Biochemistry* **1990**, *29*, 7381–7386.

(6) (a) Koga, H.; Sagara, Y.; Yaoi, T.; Tsujimura, M.; Nakamura, K.; Sekimizu, K.; Makino, R.; Shimada, H.; Ishimura, Y.; Yura, K.; Go, M.; Ikeguchi, M.; Horiuchi, T. *FEBS Lett.* **1993**, *331*, 109–113. (b) Nakamura, K.; Horiuchi, T.; Yasukochi, T.; Sekimizu, K.; Hara, T.; Sagara, Y. *Biochim. Biophys. Acta* **1994**, *1207*, 40–48. (c) Unno, M.; Shimada, H.; Toba, Y.; Makino, R.; Ishimura, Y. *J. Biol. Chem.* **1996**, *271*, 17869–17874.

effector role, some spectroscopic studies on the P450<sub>cam</sub>/Pd complex have shown that the heme active site of P450<sub>cam</sub> is influenced by Pd.<sup>8</sup> For example, the EPR study of Lipscomb showed that the complex formation shifts the spin-state equilibrium of ferric P450<sub>cam</sub> to the low-spin state.<sup>8a</sup> Shiro et al. performed a <sup>15</sup>N NMR study for the cyanide (C<sup>15</sup>N<sup>-</sup>) adduct of ferric P450<sub>cam</sub>.<sup>8c</sup> Pd caused the <sup>15</sup>N NMR signal change from 500 to 477 ppm. These observations indicate that the complexation produces observable alterations in the heme environment. This is in clear contrast to the case of the cytochrome *c* peroxidase/cytochrome *c* complex, where no observable spectral alterations in the heme environment of either protein was found.<sup>9</sup> However, we do not know how Pd perturbs the active site of P450<sub>cam</sub>. To obtain information concerning the molecular mechanism of the complexation effects, we apply resonance Raman spectroscopy to the P450<sub>cam</sub>/Pd complex and make detailed comparisons to the uncomplexed enzyme.

Resonance Raman spectroscopy is a powerful technique for probing the active site of heme proteins. Previous resonance Raman studies of P450<sub>cam</sub> have shown that the Fe–S stretching mode is observed at 351 cm<sup>-1</sup> when the S → Fe charge transfer bands are excited.<sup>10,19</sup> This Fe–S mode is an ideal measure of the heme environment, especially the heme–protein linkage at the proximal side. On the other hand, the high-frequency region of the resonance Raman spectrum is dominated by in-plane porphyrin skeletal modes.<sup>11</sup> Raman bands in this region provide information regarding the iron spin and ligation state via the changes in porphyrin conformation and electronic structure induced by the axial ligand(s). In this study, we perform resonance Raman investigations of ferric P450<sub>cam</sub> complexed with oxidized Pd. We mainly focus on the effects of Pd binding on the Fe–S axial vibrational mode and the heme iron spin and ligation state. We also report the resonance Raman spectra of ferric P450<sub>cam</sub> in the presence of various substrate analogues, and in the presence of high salt concentrations, which probes the effect of the heme environment or protein on the Fe–S mode of P450<sub>cam</sub>.

## Experimental Procedures

**Sample Preparation.** Site-directed mutagenesis of the P450<sub>cam</sub> gene was carried out as described previously.<sup>12</sup> Wild-type, mutant P450<sub>cam</sub> enzymes and Pd were expressed in *E. coli* and purified with the published procedure.<sup>13</sup> The purified protein preparations with a RZ (A<sub>392</sub>/A<sub>280</sub>) > 1.4 were employed for the present experiments. The substrate-free form of P450<sub>cam</sub> was prepared at 4 °C by passage over a Sephadex G-25 column previously equilibrated with 50 mM Tris/HCl buffer, pH 7.4. The substrate-free eluant was then concentrated, and the buffer was changed to 100 mM potassium phosphate buffer, pH 7.4. The *d*-camphor was obtained from Sigma Chemical Co. The 2-adamantanone, norcamphor, and 3,3,5,5-tetramethylcyclohexanone (TMCH) were obtained from Aldrich Chemical Co. These substrate and substrate analogues were used without further purification. The substrate analogue-bound P450<sub>cam</sub> was formed by proper dilution of a

concentrated substrate-free protein solution into the 100 mM potassium phosphate buffer, pH 7.4, which contains each substrate analogue.

For optical absorption measurements, the P450<sub>cam</sub>/Pd complex was prepared by mixing a 1:1 molar ratio of the P450<sub>cam</sub> and Pd samples in 10 mM potassium phosphate, pH 7.4, with 1 mM camphor. This solution was then split into two samples with equal volume. One of them was used to prepare the uncomplexed mixture by adding the buffer containing 0.5 M NaCl, which dissociates the complex.<sup>14</sup> The same volume of 10 mM buffer was then added to the second sample to maintain the complex. To adjust a slight difference of protein concentration, the recorded spectra were normalized by protein absorption peak in the 250–300-nm region. The pure high- and low-spin spectrum was obtained by using an effect of potassium cation on the ferric spin-state equilibrium,<sup>15</sup> i.e., higher potassium concentration increases the fraction of high-spin state. The P450<sub>cam</sub> sample in 10 mM potassium phosphate, pH 7.4, with 1 mM camphor was split into 10 and 100 mM potassium phosphate buffers for smaller and larger fractions of high-spin state, respectively. The change in the spin-state fraction induced by K<sup>+</sup> and Pd is roughly the same, and the recorded spectra were again normalized by the protein absorption peak in the 250–300-nm region.

**Spectroscopic Measurements.** Resonance Raman spectra were obtained with a Spex 1870B spectrometer equipped with a liquid nitrogen cooled CCD detector (Princeton Instruments) and a notch filter (Kaiser Optical Systems, Inc.). All samples were excited with the 356.4-nm line available from a Coherent Innova 300 krypton ion laser. All the spectra were taken at room temperature, and the laser power was about 5 mW. Standard UV-quartz fluorimeter cuvettes (NSG Precision cells, Inc.) were used for the experiments. The noise spikes in the spectra caused by cosmic rays were removed by a commercial derivative filter software routine (Princeton Instruments, Inc.). All Raman spectra were calibrated by using neat fenchone. The accuracy of the Raman shifts are about ±1 cm<sup>-1</sup> for the absolute frequency and less than ±0.2 cm<sup>-1</sup> for relative shifts. The accuracy for our Raman setup was estimated from a statistical analysis of the Fe–His stretching mode of deoxyhemoglobin, and the details are described elsewhere.<sup>16</sup> The resonance Raman spectra of the standard sample, such as the wild-type enzyme, were taken both before and after a series of Raman measurements to ensure the accuracy and reproducibility of the data. UV–visible absorption spectra were recorded with a Hitachi U-3410 spectrophotometer.

The peak positions in the Raman spectra are measured by fitting the data with Lorentzian line shapes and linear background with use of a nonlinear least-squares fitting routine.

## Results

**Effects of Putidaredoxin on the Spin Equilibrium of Ferric P450<sub>cam</sub>.** Figure 1A compares the optical absorption spectra of camphor-bound ferric P450<sub>cam</sub>/oxidized Pd complex and the uncomplexed mixture (0.5 M NaCl). Complexation decreases the absorbance around 390 nm and increases the absorbance around 420 nm, and the difference spectrum between the complex and mixture is illustrated by trace a in Figure 1C. This Pd effect has been observed previously<sup>17</sup> and serves as an indicator of complex formation. Figure 1B shows absorption changes of camphor-bound ferric P450<sub>cam</sub> induced by a different concentration of potassium cation.<sup>15</sup> As can be seen from the figure, the high- to low-spin state change is characterized by a decrease and increase in absorption around 390 and 420 nm, respectively. In Figure 1C, we also show a difference spectrum between high-spin and low-spin ferric P450<sub>cam</sub> (trace b), whose absorption maxima are at 392 and 418 nm, respec-

(7) Lipscomb, J. D.; Sligar, S. G.; Namtvedt, M. J.; Gunsalus, I. C. *J. Biol. Chem.* **1976**, *251*, 1116–1124.

(8) (a) Lipscomb, J. D. *Biochemistry* **1980**, *19*, 3590–3599. (b) Makino, R.; Iizuka, T.; Ishimura, Y.; Uno, T.; Nishimura, Y.; Tsuboi, M. In *Proceedings of the Ninth International Conference on Raman Spectroscopy*; The Chemical Society of Japan: Tokyo, 1984; pp 492–493. (c) Shiro, Y.; Iizuka, T.; Makino, R.; Ishimura, Y.; Morishima, I. *J. Am. Chem. Soc.* **1989**, *111*, 7707–7711.

(9) Wang, J.; Larsen, R. W.; Moench, S. J.; Satterlee, J. D.; Rousseau, D. L.; Ondrias, M. R. *Biochemistry* **1996**, *35*, 453–463.

(10) Champion, P. M.; Stallard, B. R.; Wagner, G. C.; Gunsalus, I. C. *J. Am. Chem. Soc.* **1982**, *104*, 5469–5472.

(11) Spiro, T. G. In *Biological Applications of Raman Spectroscopy*; Spiro, T. G., Ed.; John Wiley & Son: New York, 1988; Vol. 3, pp 1–37.

(12) Gerber, N. C.; Sligar, S. G. *J. Biol. Chem.* **1994**, *269*, 4260–4266.

(13) Gunsalus, I. C.; Wagner, G. C. *Methods Enzymol.* **1978**, *52*, 166–188.

(14) Hintz, M. J.; Mock, D. M.; Peterson, L. L.; Tuttle, K.; Peterson, J. A. *J. Biol. Chem.* **1982**, *257*, 14324–14332.

(15) Deprez, E.; Di Primo, C.; Hui Bon Hoa, G.; Douzou, P. *FEBS Lett.* **1994**, *347*, 207–210.

(16) Christian, J. F.; Unno, M.; Sage, J. T.; Chien, E.; Sligar, S. G.; Champion, P. M. *Biochemistry* In press.

(17) Sligar, S. G. Ph.D. Dissertation, 1975, University of Illinois at Urbana–Champaign.

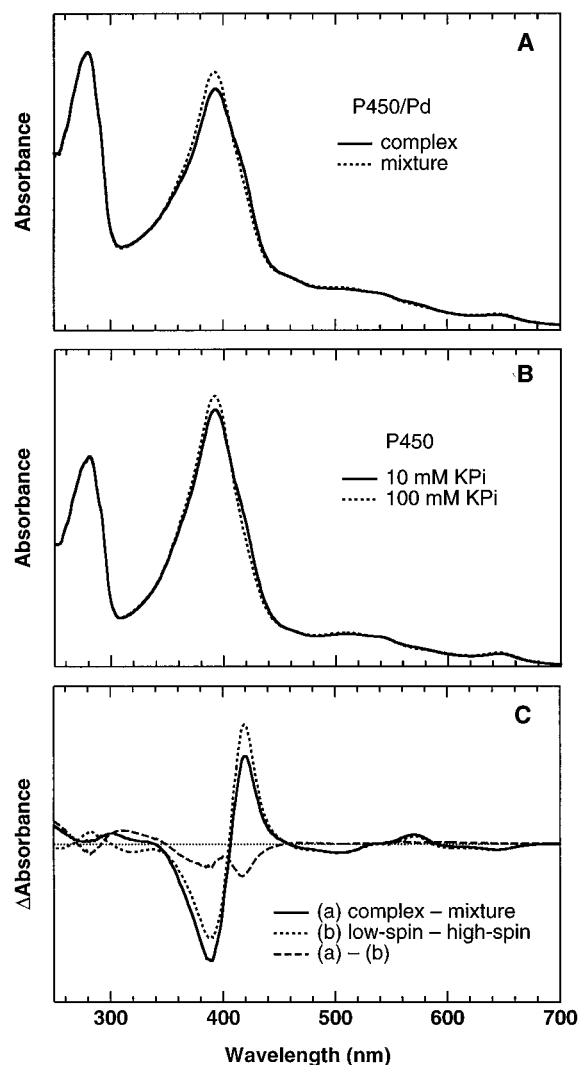


**Figure 1.** Optical absorption spectra of ferric camphor-bound P450<sub>cam</sub> and its complex with oxidized putidaredoxin. (A) Absorption spectra that compare an uncomplexed mixture to the complexed form of P450<sub>cam</sub>/putidaredoxin (1:1 ratio). The buffer was 10 mM potassium phosphate containing 1 mM camphor, pH 7.4, with (mixture) and without (complex) 0.5 M NaCl. (B) Absorption spectra of P450<sub>cam</sub> in 10 and 100 mM potassium phosphate containing 1 mM camphor, pH 7.4. The sample in 100 mM potassium phosphate buffer shows a larger fraction of high-spin state. (C) The solid line is the difference spectrum of the complexed minus the uncomplexed mixture of the two proteins (trace a). This spectrum is multiplied by a factor of 10 relative to the spectra of panel A. The difference spectrum of low-spin minus high-spin ferric P450<sub>cam</sub> is shown by the dotted line (trace b), which is normalized to the solid line between 500 and 700 nm. The difference between traces a and b is shown by the dashed line.

tively.<sup>13</sup> The complex–mixture difference spectrum is similar to the low-spin minus high-spin spectrum: both spectra are characterized by a maximum at 419 nm and a minimum at 389 nm, indicating that Pd induces spin-state shift from high spin to low spin. This conclusion is consistent with the previous EPR study of Lipscomb, where a Pd-induced production of low-spin P450<sub>cam</sub> was observed.<sup>8a</sup> However, the difference spectrum between the complex and mixture is slightly, but distinctly, different from the K<sup>+</sup>-induced high- to low-spin change. This difference can be seen in the difference of traces a and b. Note that the observed difference, in principle, can be due to changes in the optical spectra of both P450<sub>cam</sub> and Pd, and we cannot separate each contribution to the spectrum.

In Figure 2, we illustrate the high-frequency region of resonance Raman spectra of ferric P450<sub>cam</sub>. The most prominent

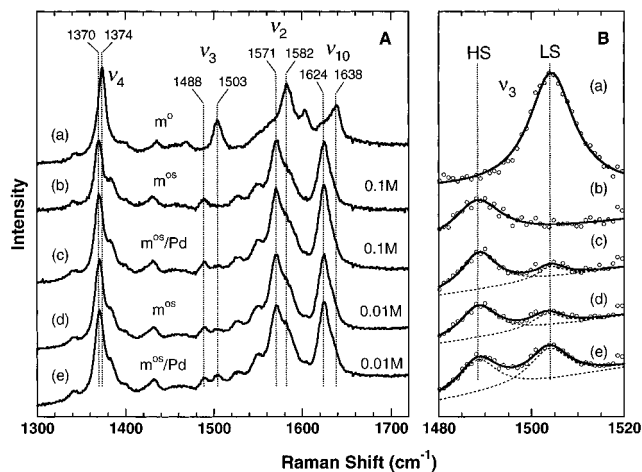


**Figure 2.** Resonance Raman spectra of ferric P450<sub>cam</sub> and its complex (1:1 ratio) with oxidized putidaredoxin (Pd) in the (A) high-frequency and (B)  $\nu_3$  spin-state marker regions. Spectrum a is that of substrate-free P450<sub>cam</sub> ( $m^0$ ) in 100 mM potassium phosphate buffer, pH 7.4. Traces b and d are the spectra of camphor-bound P450<sub>cam</sub> ( $m^{0s}$ ) in 100 mM and 10 mM potassium phosphate buffer with 1 mM camphor, pH 7.4, respectively. The spectra of P450<sub>cam</sub> complexed with Pd in 100 and 10 mM potassium phosphate buffer with 1 mM camphor, pH 7.4, are shown by traces c and e, respectively. The line shapes around the  $\nu_3$  region are fit by using two independent Lorentzians on a linear base line. The error for the peak fitting was  $\pm 0.2$  and  $\pm 0.5$   $\text{cm}^{-1}$  for the high-spin and low-spin Raman bands, respectively. All the spectra were obtained with 356.4-nm excitation with a laser power of  $\sim 5$  mW at the sample.

Raman bands in this region are heme skeletal modes, such as  $\nu_4$ ,  $\nu_3$ ,  $\nu_2$ , and  $\nu_{10}$ , whose frequencies are correlated with the electronic configuration and ligation state of the heme.<sup>11</sup> Upon binding camphor to substrate-free P450<sub>cam</sub>, these modes undergo significant changes, as seen in Figure 2A (spectra a  $\rightarrow$  b). Among these skeletal modes, the  $\nu_3$  peak, whose position is sensitive to the iron spin state and porphyrin core size,<sup>11</sup> is well resolved from other heme vibrational modes. Figure 2B shows expanded plots of the  $\nu_3$  region of the Raman spectra as well as the peak-fitting results. The  $\nu_3$  mode in substrate-free P450<sub>cam</sub> is at 1503  $\text{cm}^{-1}$ , consistent with a six-coordinate low-spin (6C/LS) state in which both the thiolate sulfur of Cys357 and a water molecule are coordinated to the heme iron.<sup>18</sup> In the camphor-bound protein, the  $\nu_3$  mode downshifts to 1488  $\text{cm}^{-1}$ , indicating a five-coordinate high-spin (5C/HS) state in which the iron-coordinated water molecule has been expelled. Figure 2 also compares camphor-bound P450<sub>cam</sub> (traces b and d) and its complex with Pd (traces c and e) under different buffer concentrations. Because the oxidized Pd does not show any Raman bands in this region, the observed changes are attributable to P450<sub>cam</sub>. Spectra b and c were obtained in 100 mM potassium phosphate, and the  $\nu_3$  mode at 1503  $\text{cm}^{-1}$  for the 6C/LS species appeared upon complexation. Traces d and e are the spectra of free and complexed P450<sub>cam</sub>, respectively, at low ionic strength (10 mM potassium phosphate), where we can expect a higher affinity of Pd for P450<sub>cam</sub>.<sup>14</sup> Under these conditions, the concentration of K<sup>+</sup> is low and the  $\nu_3$  for the 6C/LS (1503  $\text{cm}^{-1}$ ) mode is present even in the absence of Pd.<sup>15</sup> The binding of Pd, however, increases the intensity of the 1503- $\text{cm}^{-1}$  mode. The result of Figure 2 is consistent with the data of Figure 1, where we showed the Pd-induced spin-state shift to low-spin form in the absorption spectra. Furthermore, a peak fitting analysis (Figure 2B) demonstrates that the frequency for

(18) (a) Poulos, T. L.; Finzel, B. C.; Howard, A. J. *Biochemistry* **1986**, *25*, 5314–5322. (b) Thomann, H.; Bernardo, M.; Goldfarb, D.; Kroneck, P. M. H.; Ullrich, V. *J. Am. Chem. Soc.* **1995**, *117*, 8243–8251.

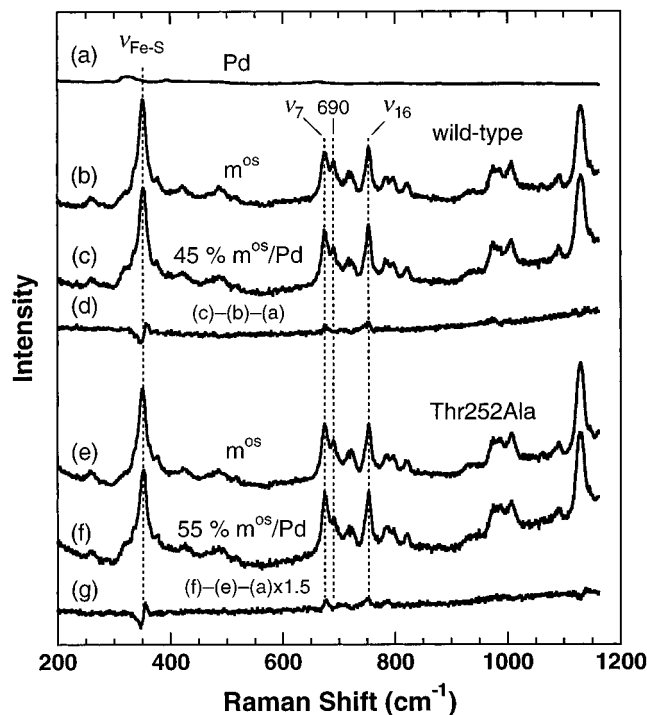


**Figure 3.** Low-frequency region of resonance Raman spectra of (a) oxidized putidaredoxin, (b) wild-type ferric P450<sub>cam</sub>, (c) P450<sub>cam</sub>–putidaredoxin complex, and (e) Thr252Ala ferric P450<sub>cam</sub> and (f) its diprotein complex with putidaredoxin in 100 mM potassium phosphate buffer with 1 mM camphor, pH 7.4. The following list gives the protein concentration and the fraction of the complex formation for spectra c and f: (c) [P450] = 0.42 mM, [Pd] = 0.27 mM, 45%; (f) [P450] = 0.29 mM, [Pd] = 0.27 mM, 55%. The difference spectrum for wild-type enzyme [(c) – (b) – (a)] is shown in trace d, and a corresponding difference spectrum for Thr252Ala mutant [(f) – (e) – (a) × 1.5] is shown in trace g. The Pd spectrum is normalized by minimizing its contribution to the difference spectra of traces d and g. The fitting analysis estimates the  $\nu_{\text{Fe-S}}$  shift as  $+1.1 \pm 0.2$  and  $+1.4 \pm 0.2$   $\text{cm}^{-1}$  for wild-type and Thr252Ala mutant, respectively. The other experimental conditions are the same as those given in Figure 2.

the Pd-induced  $\nu_3$  mode is indistinguishable from that of substrate-free P450<sub>cam</sub>.

**Effects of Putidaredoxin on the Fe–S Stretching Mode of P450<sub>cam</sub>.** The upper three spectra in Figure 3 show the low frequency region of the resonance Raman spectra for oxidized Pd, ferric camphor-bound P450<sub>cam</sub>, and their diprotein complex. The intense Raman band at  $351 \text{ cm}^{-1}$  has been assigned to the Fe–S stretching mode in P450<sub>cam</sub>.<sup>10</sup> Further studies have established that this mode is coupled to  $\text{S} \rightarrow \text{Fe}$  charge transfer excitations near 320 and 360 nm, which are present only in the 5C/HS form.<sup>19</sup> The difference spectrum (trace d) clearly demonstrates that the binding of Pd upshifts the Fe–S mode. Only part of the P450<sub>cam</sub> population is complexed with Pd in this experiment, because of the relatively low Pd concentration. This leads to an overall line-shape function of the observed Fe–S mode that is a superposition of two Raman bands, which originate from complexed and uncomplexed materials. For small shifts, it is a good approximation to take the overall line shape to be one Lorentzian function having a peak position that depends linearly on the amount of complexed P450<sub>cam</sub>. We can estimate the fraction of complex formation using the reported dissociation constant for ferric P450<sub>cam</sub>/oxidized Pd complex ( $K_d = 0.1 \text{ mM}$ ).<sup>14</sup> This allows us to extrapolate that

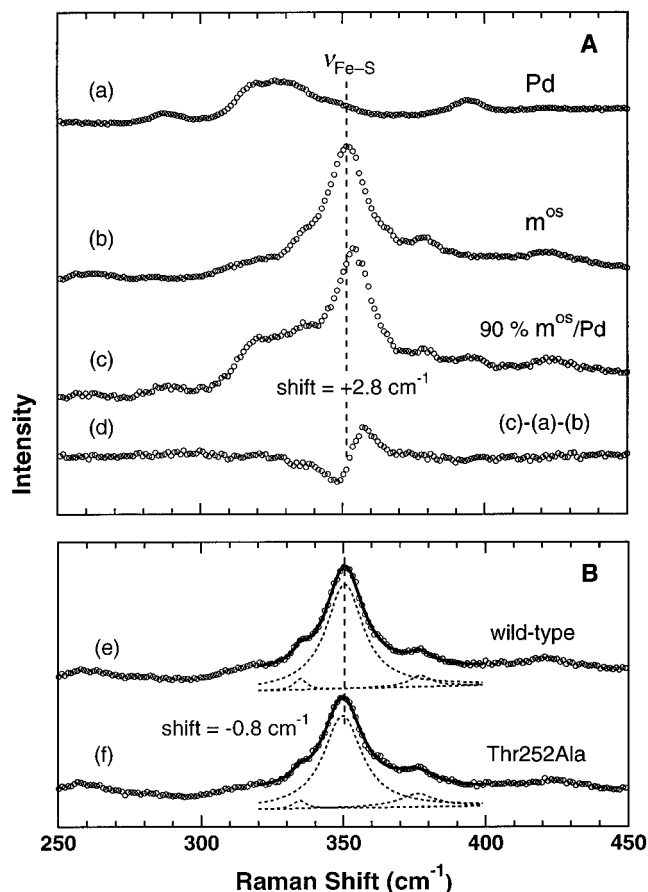


**Figure 4.** Resonance Raman spectra of ferric camphor-bound P450<sub>cam</sub> and oxidized putidaredoxin, in the Fe–S stretching mode region. (A) Traces a and b are the spectra of putidaredoxin and wild-type P450<sub>cam</sub>, respectively, and the spectrum for their diprotein complex is shown in trace c. The protein concentration for spectra c is as follows: [P450] = 0.5 mM, [Pd] = 1.1 mM. A 100 mM potassium phosphate buffer with 1 mM camphor, pH 7.4, was used. The difference spectrum (c) – (a) – (b) is shown in trace d. (B) Traces e and f are the spectra of ferric wild-type and Thr252Ala mutant enzymes, respectively, in 10 mM potassium phosphate buffer with 1 mM camphor, pH 7.4. The line shapes around the  $351 \text{ cm}^{-1}$  Fe–S mode region are fit by using three independent Lorentzians on a linear base line. The other experimental conditions are the same as those given in Figure 2.

the Pd binding shifts the Fe–S mode by  $\sim 3 \text{ cm}^{-1}$  for 100% complexation.<sup>20</sup> This estimation is confirmed by an experiment with a larger amount of Pd (Figure 4A). We used  $\sim 2$ -fold excess Pd in this latter experiment (90% complex formation) and observed a  $2.8 \pm 0.2 \text{ cm}^{-1}$  upshift. These results are summarized in Table 1. In addition to the effect on the Fe–S mode, Pd increases the intensity of the  $\nu_7$  ( $674 \text{ cm}^{-1}$ ) and  $\nu_{16}$  ( $753 \text{ cm}^{-1}$ ) modes (Figure 3). Because substrate-free P450<sub>cam</sub> (6C/LS) exhibits larger  $\nu_7$  and  $\nu_{16}$  modes than the camphor-bound form (5C/HS) (data not shown), this effect can be explained by the spin-state equilibrium shift from high to low spin.

The bottom three spectra of Figure 3 are a set of data for the Thr252 → Ala mutant of P450<sub>cam</sub>. The crystal structure of

(20) For a simple bimolecular binding equilibrium between P450<sub>cam</sub> and Pd, i.e.,  $\text{P450} + \text{Pd} \leftrightarrow \text{P450/Pd}$ , the complex formation fraction,  $f_{\text{complex}}$ , can be expressed as follows:  $f_{\text{complex}} = \{([\text{P450}] + [\text{Pd}] + K_d) - ([\text{P450}] + [\text{Pd}] + K_d)^2 - 4[\text{P450}][\text{Pd}]\}^{0.5} / 2[\text{P450}]$ , where [P450] and [Pd] are total concentrations of P450<sub>cam</sub> and Pd, respectively. The observed Fe–S stretching frequency can be approximated as  $\nu_{\text{Fe-S(obs)}} = f_{\text{complex}} \nu_{\text{Fe-S(P450/Pd)}} + (1 - f_{\text{complex}}) \nu_{\text{Fe-S(P450)}}$ , where  $\nu_{\text{Fe-S(P450/Pd)}}$  and  $\nu_{\text{Fe-S(P450)}}$  are the Fe–S frequency for the complexed and uncomplexed enzymes, respectively. All the observed Pd-induced shifts extrapolate to  $\sim 3 \text{ cm}^{-1}$  for 100% complexation with use of these equations.

(19) (a) Bangcharoenpaupong, O.; Champion, P. M.; Martinis, S. A.; Sligar, S. G. *J. Chem. Phys.* **1987**, *87*, 4273–4284. (b) Champion, P. M. *J. Am. Chem. Soc.* **1989**, *111*, 3433–3434.

**Table 1.** Summary of the Fe–S Stretching Frequency for the Ferric Cytochrome P450<sub>cam</sub><sup>a</sup>

sample	$\nu_{\text{Fe-S}}$ (cm <sup>-1</sup> )	shift (cm <sup>-1</sup> ) <sup>b</sup>
(I) Effect of Putidaredoxin on Wild-Type P450 <sub>cam</sub>		
P450	350.5	
P450/Pd (45% complex) <sup>c</sup>	351.6	+1.1
P450/Pd (90% complex) <sup>c</sup>	353.3	+2.8
P450/Pd (extrapolation) <sup>d</sup>		+3
(II) Effect of Putidaredoxin on Thr252Ala Mutant P450 <sub>cam</sub>		
P450	349.7	
P450/Pd (55% complex) <sup>c</sup>	351.1	+1.4
P450/Pd (extrapolation) <sup>d</sup>		+3
(III) Effect of Substrate and Substrate Analogues		
camphor	350.5	
adamantanone	350.5	<0.2
norcamphor	349.7	-0.8
TMCH <sup>e</sup>	349.4	-1.1
(IV) Effect of Solvent Composition		
buffer	351.0	
+ 40% glycerol	351.0	<0.2
+ 1 M NaCl	351.5	+0.5
+ 0.5 M (NH <sub>4</sub> ) <sub>2</sub> SO <sub>4</sub>	351.6	+0.6

<sup>a</sup> The following list gives the buffer condition for experiments I–IV: (I,II) 100 mM potassium phosphate buffer with 1 mM camphor, pH 7.4; (III) 100 mM potassium phosphate buffer, pH 7.4 with camphor or camphor analogues; (IV) 10 mM potassium phosphate/90 mM KCl buffer, pH 7.4 with or without additional solutes. <sup>b</sup> The accuracy of the shifts is less than  $\pm 0.2$  cm<sup>-1</sup>. <sup>c</sup> The fraction of P450<sub>cam</sub>/putidaredoxin complex was estimated by using  $K_d = 0.1$  mM. The details are described in footnote 20. <sup>d</sup> Extrapolation for 100% complexation. See text for details. <sup>e</sup> 3,3,5,5-Tetramethylcyclohexanone.

P450<sub>cam</sub> shows that the distal Thr252 residue is located in the immediate vicinity of the heme active site.<sup>21</sup> Thr252 is one of the most conserved amino acid residues for the cytochrome P450 family<sup>22</sup> and is thought to play an important role in P450 catalysis.<sup>23</sup> As can be seen from Figure 3, Pd binding also upshifts the Fe–S mode for the Thr252Ala mutant (Table 1). With use of the same  $K_d$  for wild-type, we can extrapolate that the Fe–S mode is upshifted by  $\sim 3$  cm<sup>-1</sup> for 100% complexation.

Although we observed no difference between the wild-type and Thr252Ala mutant for the Pd-induced shift of the Fe–S mode, the resonance Raman spectrum of this mutant is slightly different from that of wild-type. The  $\nu_{\text{Fe-S}}$ ,  $\nu_7$ , and  $\nu_{16}$  peak intensity is perturbed by the mutation. For example, the relative intensity of the  $\nu_7$  to its shoulder peak at 690 cm<sup>-1</sup> is increased. Because the optical absorption measurement shows that this mutant exhibits a slightly larger low-spin fraction compared to the wild-type (not shown), these changes in relative intensity can be interpreted in terms of the spin-state change. Another influence of the mutation is that the frequency of the Fe–S mode is downshifted (0.8 cm<sup>-1</sup>), as shown in Figure 4B.

**Substrate- and Salt-Induced Shift of the Fe–S Stretching Frequency.** The crystal structure of camphor-bound P450<sub>cam</sub> shows that the camphor molecule is buried in an internal pocket just above the heme distal surface adjacent to the ligand binding site.<sup>21</sup> Many spectroscopic studies have revealed that the binding of camphor, and its analogues, causes drastic changes in the heme environment and its electronic structure. For ferric P450<sub>cam</sub>, camphor binding displaces waters from the distal pocket, changing the heme iron from a 6C/LS configuration with water as an axial ligand to a 5C/HS configuration. Upon

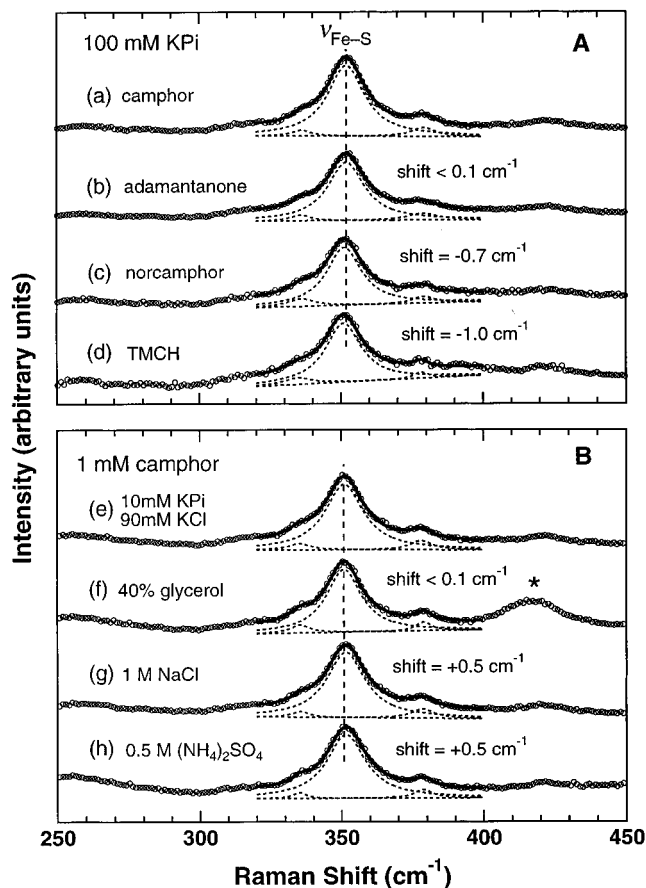


**Figure 5.** Resonance Raman spectra of wild-type ferric P450<sub>cam</sub> in the Fe–S stretching mode region with camphor and camphor analogues. Panel A demonstrates spectra in 100 mM potassium phosphate buffer, pH 7.4, with (a) 1 mM *d*-camphor, (b) 1 mM 2-adamantanone, (c) 3 mM norcamphor, and (d) 1.4 mM 3,3,5,5-tetramethylcyclohexanone (TMCH). Panel B shows spectra in 10 mM potassium phosphate/90 mM KCl buffer with 1 mM camphor, pH 7.4, containing (e) no additional salts, (f) 40% (w/w) glycerol, (g) 1 M NaCl, and (h) 0.5 M (NH<sub>4</sub>)<sub>2</sub>SO<sub>4</sub>. The asterisk indicates a Raman band of glycerol. The line shapes around the 351 cm<sup>-1</sup> Fe–S mode region are fit by using three independent Lorentzians on a linear base line. The other experimental conditions are the same as those given in Figure 2.

binding different substrate analogues, P450<sub>cam</sub> exists in varying proportions of high- and low-spin forms. For example, the binding of norcamphor and TMCH is characterized by a 45 and 14% high-spin fraction, respectively, whereas the high-spin fraction of adamantanone-bound enzyme (99%) is comparable to that of the camphor complex (95%).<sup>24</sup> X-ray analysis of P450<sub>cam</sub> with various substrate analogues indicates that the presence of water in the heme pocket is correlated with the ferric spin-state equilibrium of the enzyme;<sup>25</sup> a larger degree of hydration in the heme pocket corresponds to a larger amount of the low-spin form. Figure 5A shows the effect of camphor analogues on the Fe–S mode. Because this mode is only present in the high-spin P450<sub>cam</sub>, its intensity in the spectra of both norcamphor and TMCH-bound enzymes is reduced. The normalization of the Fe–S mode is arbitrary in this figure. As can be seen, the replacement of the substrate, from camphor to adamantanone, has little effect on the Fe–S stretching frequency. In contrast, the frequency of the Fe–S mode is slightly downshifted in the norcamphor and TMCH complexes. Peak-fitting analysis yields  $-0.8$ - and  $-1.1$ -cm<sup>-1</sup> shifts for norcamphor and TMCH, respectively (Table 1). Because the order of

(21) Poulos, T. L.; Finzel, B. C.; Howard, A. J. *J. Mol. Biol.* **1987**, *195*, 687–700.

(22) Nelson, D. R.; Strobel, H. W. *Biochemistry* **1989**, *28*, 656–660.

(23) (a) Imai, M.; Shimada, H.; Watanabe, Y.; Matsushima-Hibiya, Y.; Makino, R.; Koga, H.; Horiuchi, T.; Ishimura, Y. *Proc. Natl. Acad. Sci. U.S.A.* **1989**, *86*, 7823–7827. (b) Martinis, S. A.; Atkins, W. M.; Stayton, P. S.; Sligar, S. G. *J. Am. Chem. Soc.* **1989**, *111*, 9252–9253.

(24) Fisher, M. T.; Sligar, S. G. *Biochemistry* **1985**, *24*, 6696–6701.

(25) Raag, R.; Poulos, T. L. *Biochemistry* **1991**, *30*, 2674–2684.

the shift is roughly proportional to the fraction of low spin, we correlate this  $\nu_{\text{Fe-S}}$  shift to the extent of water present in the pocket. This conclusion is qualitatively consistent with the data shown in Figure 4B. We observed a  $0.8\text{-cm}^{-1}$  downshift for Thr252Ala mutant, whose optical spectrum indicates a slightly larger low-spin fraction and whose crystal structure shows a presence of water in the pocket.<sup>26</sup>

We have also examined the effect of solvent composition on the Fe-S mode (Figure 5B). We used 10 mM potassium phosphate/90 mM KCl buffer for the reference sample and examined the effect of glycerol (f), NaCl (g), and  $(\text{NH}_4)_2\text{SO}_4$  (h). These solutions show no spectral features in the region between 300 and  $400\text{ cm}^{-1}$ . Figure 5B demonstrates that the Fe-S mode is upshifted by  $\sim 0.5\text{ cm}^{-1}$  in the presence a high salt concentration (Table 1). Because the addition of the salts has little effect on the ferric high-to-low spin equilibrium of P450<sub>cam</sub>, the observed shift of the Fe-S mode is not correlated with a salt-induced spin transition. In fact, the absence of an effect of glycerol on the Fe-S mode excludes this possibility since Di Primo et al. reported that glycerol increases the fraction of high-spin P450<sub>cam</sub>.<sup>27</sup>

## Discussion

The P450<sub>cam</sub>-Pd couple is one of the best-studied systems of biological electron transfer. On the basis of competitive inhibition of the cytochrome *b*<sub>5</sub> binding to P450<sub>cam</sub> by Pd, as well as the molecular modeling of the cytochrome *b*<sub>5</sub>/P450<sub>cam</sub> complex, Stayton et al. suggested that the basic P450<sub>cam</sub> residues Arg72, Arg112, Lys344, and Arg364 form electrostatic interactions with Pd.<sup>4</sup> The distribution of these charged residues directly above the proximal cysteine ligand makes the proximal face of the molecule positive. Because Pd carries a strong negative charge, close approach of Pd to the proximal face is expected to be favored by charge interactions. Subsequent site-directed mutagenesis of the above P450<sub>cam</sub> residues confirms the involvement of the proximal face in forming the diprotein complex.<sup>5,6</sup> With the availability of P450<sub>cam</sub> and Pd structures, Pochapsky et al. recently proposed the P450<sub>cam</sub>/Pd complex structure.<sup>28</sup> This model shows a  $12\text{ \AA}$  Fe-Fe distance, with three residues Arg109, Arg112, and Arg79 of P450<sub>cam</sub> forming salt bridges with Pd Asp34, Asp38, and Trp106 carboxylate, respectively. These intensive investigations provide a strong structural basis for interpreting the present and previous spectroscopic data.

**Effects of Complexation on the Spin Equilibrium of Ferric P450<sub>cam</sub>.** The optical absorption (Figure 1) and resonance Raman (Figure 2) studies confirm previous results that Pd shifts the spin-state equilibrium of ferric P450<sub>cam</sub> to the low-spin form.<sup>8a,17</sup> The data shown in Figure 1 further demonstrate that the Pd-induced difference spectrum is slightly different from the  $\text{K}^+$ -induced high-spin to low-spin difference spectrum. The latter observation implies that complexation causes some additional changes in the active sites of P450<sub>cam</sub> and/or Pd beyond the  $\text{K}^+$ -induced spin-state change of P450<sub>cam</sub>. Similar effects associated with Pd binding have been reported by Lipscomb,<sup>8a</sup> who measured the EPR spectrum of the P450<sub>cam</sub>/Pd complex and found an appearance of a new low-spin signal in the complex. These findings raise the possibility that Pd produces an unusual low-spin species, such as five-coordinate low-spin heme (5C/LS). Although low-spin heme is usually a

six-coordinate complex, English et al. successfully prepared a 5C/LS heme compound: ferric porphyrin complex with a hydrosulfido ( $\text{SH}^-$ ) axial ligand.<sup>29</sup> The high-frequency resonance Raman data of Figure 2, however, show that the  $\nu_3$  position of the Pd-induced low-spin species is indistinguishable from that of a water-coordinated 6C/LS enzyme, i.e., substrate-free P450<sub>cam</sub>. Because the frequency of the  $\nu_3$  mode is highly sensitive to the iron spin state and the geometry of the porphyrin macrocycle, we attribute the Pd-induced low-spin species to the usual six-coordinate heme.

The most likely explanation for the increased low-spin population upon Pd complexation involves a distal pocket structural change that allows water to enter the heme pocket. The high-spin to low-spin equilibrium of ferric P450<sub>cam</sub> is very sensitive to the distal pocket structure. For example, optical absorption measurements show that replacement of Thr252 by Ala results in a small increase in the low-spin fraction (not shown). In fact, the X-ray structure of this mutant shows that a water molecule, which is not present in the wild-type enzyme, is positioned in the heme pocket.<sup>26</sup> Mutations of the other distal pocket residues, such as Tyr96, Thr101, Thr185, Val247, and Val295, also affect the spin-state equilibrium.<sup>30</sup> Small structural changes at the distal side could be enough to alter the partial occupancy of water at the iron site and, thus, the spin state of the ferric enzyme, even though Pd is expected to bind the proximal face of P450<sub>cam</sub>.

It is of interest to compare the effects of Pd on the spin equilibrium of P450<sub>cam</sub> with those in mitochondrial cytochrome P450<sub>sec</sub>. A Pd-like iron-sulfur protein, adrenodoxin, transports electrons to P450<sub>sec</sub> in this system. In contrast to the P450<sub>cam</sub>/Pd couple, the binding of adrenodoxin shifts the spin-state equilibrium to the high-spin form.<sup>31</sup>

**Origin of the Putidaredoxin-Induced Shift of the Fe-S Stretching Mode.** The high-frequency resonance Raman data (Figure 2) show no detectable effect of Pd on the  $\nu_3$  position for high-spin P450<sub>cam</sub>, although the spin-state equilibrium is shifted. This observation indicates that no gross structural changes in the high-spin heme are incurred by the complexation. However, the low-frequency resonance Raman spectra (Figures 3 and 4, Table 1) demonstrate that Pd upshifts the Fe-S stretching mode by  $\sim 3\text{ cm}^{-1}$ . These results are understandable because the Fe-S mode is perpendicular to the in-plane heme modes and is expected to be sensitive to different perturbations of the heme and the surrounding pocket. We discuss possible mechanisms of the Pd-induced shift of the Fe-S mode below.

In the previous section, we suggested that Pd complexation increases water access to the heme, which results in the formation of the low-spin enzyme. If noncoordinated water is present in the heme pocket of the P450<sub>cam</sub>/Pd complex, such water may also affect the Fe-S mode of P450<sub>cam</sub>. Recent <sup>1</sup>H NMR<sup>32</sup> and resonance Raman<sup>16</sup> investigations of distal pocket mutants of deoxymyoglobin suggest that the presence or absence of water in the heme pocket affects the heme iron-proximal histidine bonding character. To test for the effect of pocket hydration on the Fe-S stretching frequency, we examined the  $\nu_{\text{Fe-S}}$  region of the resonance Raman spectra of P450<sub>cam</sub> in the presence of various substrates. We found in Figure 5A and Table 1 that an increased amount of low spin (i.e., larger hydration) leads to a small downshift of the Fe-S mode ( $\leq 1$

(29) English, D. R.; Hendrickson, D. N.; Suslick, K. S.; Eigenbrot, C. W., Jr.; Scheidt, W. R. *J. Am. Chem. Soc.* **1984**, *106*, 7258-7259.

(30) (a) Atkins, W. M.; Sligar, S. G. *J. Biol. Chem.* **1988**, *263*, 18848-18849. (b) Loida, P. J.; Sligar, S. G. *Biochemistry* **1993**, *32*, 11530-11538.

(31) Hanukoglu, I.; Spitsberg, V.; Bumpus, J. A.; Dus, K. M.; Jefcoate, C. R. *J. Biol. Chem.* **1981**, *256*, 4321-4328.

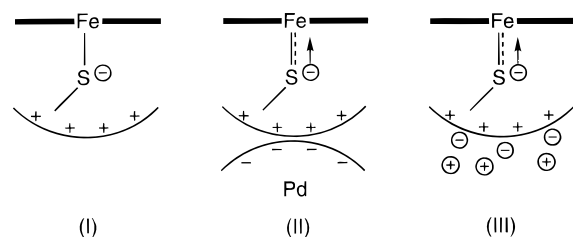
(32) La Mar, G. N.; Dalichow, F.; Zhao, X.; Dou, Y.; Ikeda-Saito, M.; Chiu, M. L.; Sligar, S. G. *J. Biol. Chem.* **1994**, *269*, 29629-29635.

(26) Raag, R.; Martinis, S. A.; Sligar, S. G.; Poulos, T. L. *Biochemistry* **1991**, *30*, 11420-11429.

(27) Di Primo, C.; Deprez, E.; Hui Bon Hoa, G.; Douzou, P. *Biophys. J.* **1995**, *68*, 2056-2061.

(28) Pochapsky, T. C.; Lyons, T. A.; Kazanis, S.; Arakaki, T.; Ratnaswamy, G. *Biochimie* **1996**, *78*, 723-733.

## Scheme 1



$\text{cm}^{-1}$ ). This observation is consistent with the  $0.8\text{-cm}^{-1}$  downshift (Figure 4B) for the Thr252Ala mutant, whose crystal structure shows a noncoordinated water in the distal pocket.<sup>26</sup> These results strongly suggest that the distal pocket water influences the Fe–S bond of P450<sub>cam</sub>; however, the direction of the shift ( $\sim 1\text{-cm}^{-1}$  downshift) is opposite to the observed  $\sim 3\text{-cm}^{-1}$  upshift for the P450<sub>cam</sub>/Pd complex (Figure 4A). Therefore, Pd-induced hydration of the distal pocket cannot be invoked to explain the Pd-induced shift of the Fe–S mode.

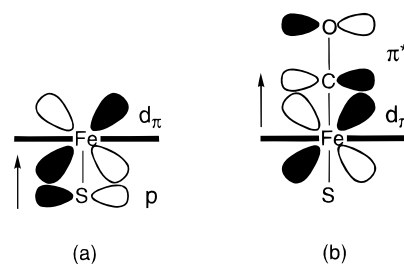
As a result, we suggest that the vibrational frequency of the Fe–S bond is perturbed by electrostatic or structural changes on the proximal side of the heme. This idea is consistent with the lack of effect of the Thr252 mutation on the Pd-induced  $\nu_{\text{Fe-S}}$  shift (Figure 3). This result implies that the effect of Pd on the Fe–S mode is not mediated by the distal pocket residue Thr252. A possible factor which may influence the Fe–S bond is charge and polar interactions. In general, these interactions can affect the electron distribution within a molecule, and thus may alter its bond order and vibrational frequency. Electrostatic modeling showed that the distribution of charged residues on the proximal face of P450<sub>cam</sub> makes the proximal side of the heme pocket positive.<sup>5</sup> As shown in Scheme 1, this positively charged environment will stabilize the negative character of the proximal thiolate anion (form I). On the other hand, when P450<sub>cam</sub> is complexed with the anionic Pd, the positive character of the proximal pocket should be diminished. The thiolate anion will be destabilized in this situation, and the S  $\rightarrow$  Fe electron donation could be enhanced (form II). This accounts for the upshifted Fe–S stretching frequency in the complex. In order to test this idea, we compared the  $\nu_{\text{Fe-S}}$  frequency in the presence and absence of high salt concentration (Figure 5B). Since the high ionic strength is expected to shield the positive charges on the proximal side, the addition of salts would promote the S  $\rightarrow$  Fe electron donation (form III). As expected, we observed an  $\sim 0.5\text{-cm}^{-1}$  upshift in the presence of 1 M NaCl or 0.5 M  $(\text{NH}_4)_2\text{SO}_4$ . Although the shift is smaller than the Pd-induced shift of  $\sim 3\text{ cm}^{-1}$ , this result is supportive of the suggestion that the protein electrostatic environment contributes to the frequency of the Fe–S mode.

**Previous Spectroscopic Studies on the P450<sub>cam</sub>/Putidaredoxin Complex.** Egawa et al. reported that the O–O stretching frequency of oxygenated P450<sub>cam</sub> is little altered by Pd binding.<sup>33</sup> However, other spectroscopic investigations have shown that the complexation of Pd perturbs the heme active site of P450<sub>cam</sub>. Makino et al. measured IR and resonance Raman spectra of ferrous CO–P450<sub>cam</sub> in the presence and absence of Pd and found that the stretching frequency of the C–O mode is downshifted from 1940 to 1932  $\text{cm}^{-1}$  upon the Pd binding, while that of Fe–CO mode is upshifted from 481 to 483  $\text{cm}^{-1}$ .<sup>8b</sup> Similar influences on the C–O and Fe–CO modes have been reported for adrenodoxin binding to cytochrome P450<sub>sc</sub>.<sup>34</sup> Although the magnitudes of the shifts are smaller for cytochrome

(33) Egawa, T.; Ogura, T.; Makino, R.; Ishimura, Y.; Kitagawa, T. *J. Biol. Chem.* **1991**, *266*, 10246–10248.

(34) Tsubaki, M.; Yoshikawa, S.; Ichikawa, Y.; Yu, N.-Y. *Biochemistry* **1992**, *31*, 8991–8999.

## Scheme 2



P450<sub>sc</sub>, the direction of the frequency shift upon complexation is the same. Shiro et al.<sup>8c</sup> demonstrated that the Pd binding to ferric C<sup>15</sup>N-bound P450<sub>cam</sub> decreases the <sup>15</sup>N NMR shift from 500 to 477 ppm, indicating a decrease of electron spin density on the <sup>15</sup>N atom. These results are consistent with the present finding that the Pd binding increases the Fe–S stretching frequency. If, for example, we assume the proximal cysteine residue is  $sp^2$  hybridized to account for anisotropic EPR  $g$  values as previously suggested,<sup>10,19a</sup> a Pd-induced increase in the Fe–S bond order can be explained in terms of an enhanced electron donation from S  $\rightarrow$  Fe through a  $\pi$ -bonding interaction between a sulfur p-orbital and Fe  $d_{\pi}$  orbital (Scheme 2, a). The enhanced electron donation due to the Pd binding implies an increased electron density in the Fe  $d_{\pi}$  orbital, which would result in an enhanced Fe  $d_{\pi} \rightarrow$  CO  $\pi^*$  electron donation (Scheme 2, b). This accounts for the increased and decreased bond order, observed by Makino et al.,<sup>8b</sup> in the Fe–CO and C–O bonds, respectively. Analogously, the Pd binding could weaken the C–N bond of cyanide-bound P450<sub>cam</sub>, and this might explain the observed decrease in the <sup>15</sup>N NMR shift for the diprotein complex.<sup>8c</sup> These Pd effects may also be related to the “effector role” of Pd for camphor hydroxylation.<sup>7</sup> For example, the enhanced S  $\rightarrow$  Fe electron donation could stabilize the highly electrophilic reaction intermediate during the P450 catalysis, as originally suggested by Dawson and co-workers for the role of the proximal cysteine residue.<sup>35</sup>

## Conclusions

We have used resonance Raman spectroscopy to probe the effect of Pd on the heme active site of ferric camphor-bound P450<sub>cam</sub>. We find that Pd binding produces a six-coordinate low-spin species, with water as the probable sixth ligand. This result suggests that the Pd binding affects the distal side of P450<sub>cam</sub> and increases the water occupancy of the pocket. We also demonstrate that Pd binding upshifts the Fe–S mode by  $\sim 3\text{ cm}^{-1}$ . Investigations of the Fe–S mode with a distal pocket mutant, substrate analogues, and salts suggest that positive charge located on the proximal face is one of the determinants of the Fe–S stretching frequency. Because the proximal face of P450<sub>cam</sub> is the proposed Pd docking site, we suggest that the negatively charged character of the Pd screens the proximal positive charges on P450<sub>cam</sub> and promotes sulfur  $\rightarrow$  iron electron donation, which accounts for the increased Fe–S stretching frequency.

**Acknowledgment.** This work was supported by grants from NIH DK-35090 (P.M.C.), PHS GM-31756 (S.G.S.) and PHS GM-33775 (S.G.S.), and NSF 94-05979 (P.M.C.). M.U. was a recipient of JSPS Postdoctoral Fellowship for Research Abroad. We thank T. C. Pochapsky for sending their preprint prior to its publication.

JA963785A

(35) Dawson, J. H.; Holm, R. H.; Trudell, J. R.; Barth, G.; Linder, R. E.; Bunnenberg, E.; Djerassi, C.; Tang, S. C. *J. Am. Chem. Soc.* **1976**, *98*, 3707–3709.